# Discrete Tunable Color Entanglement

S. Ramelow,[1,2] L. Ratschbacher,[1] A. Fedrizzi,[1,2,3] N. K. Langford,[1,2] and A. Zeilinger[1,2]

[1]*Institute for Quantum Optics and Quantum Information, Austrian Academy of Sciences, Boltzmanngasse 3, A-1090 Vienna, Austria*
[2]*Faculty of Physics, University of Vienna, Boltzmanngasse 5, A-1090 Vienna, Austria*
[3]*Physics Department & Centre for Quantum Computer Technology, University of Queensland, Qld 4072, Australia*

(Received 30 April 2009; published 16 December 2009)

Although frequency multiplexing of information has revolutionized the field of classical communications, the color degree of freedom (DOF) has been used relatively little for quantum applications. We experimentally demonstrate a new hybrid quantum gate that transfers polarization entanglement of nondegenerate photons onto the color DOF. We create, for the first time, high-quality, discretely color-entangled states (with energy band gap up to 8.4 THz) without any spectrally selective filtering, and unambiguously verify and quantify the amount of entanglement (tangle, $0.611 \pm 0.009$) by reconstructing a restricted density matrix; we generate a range of maximally entangled states, including a set of mutually unbiased bases for an encoded qubit space. The technique can be generalized to transfer polarization entanglement onto other photonic DOFs, like orbital angular momentum.

DOI: 10.1103/PhysRevLett.103.253601 PACS numbers: 42.50.Dv, 03.65.Wj, 03.67.Bg, 42.50.Ex

Color, or frequency, is one of the most familiar degrees of freedom (DOFs) of light and has been routinely analyzed in spectroscopy for centuries. However, although frequency multiplexing of information has had a profound impact on classical telecommunications, little work has aimed at exploiting the frequency DOF for quantum-based information technologies. A key ingredient in many such technologies is discretely encoded entanglement, which has been extensively investigated for other optical degrees of freedom (e.g., [1–9]). In contrast, discrete frequency entanglement has not yet been unambiguously demonstrated, despite potentially interesting applications such as enhanced clock synchronization beyond the classical limit [10,11], improved quantum communication in noisy channels [12], and novel dispersion cancellation techniques in quantum interferometry [13]. Flying qubits encoded in tunable frequency bins would also be an ideal mediator between stationary qubits with different energy levels; e.g., very recently the state of two photons emitted by two separate Yb ions was projected onto a discrete frequency-entangled state, allowing the creation of entanglement and realization of teleportation between the ions [14]. Finally, the higher-dimensional Hilbert space accessible with the color DOF has known benefits for quantum communication [15,16] and quantum cryptography [17–19], and would also allow the exploration of fundamental questions about quantum mechanics [20].

Continuous frequency entanglement between photon pairs arises naturally in spontaneous parametric down-conversion (SPDC) experiments as a consequence of energy conservation [5,21–23]. It is often, however, much simpler to control and use entanglement between systems with discrete, well-separated basis states (cf. time-bin entanglement [6]). A simple discrete-color-entangled state would be $(|\omega_1\rangle|\omega_2\rangle + |\omega_2\rangle|\omega_1\rangle)/\sqrt{2}$, where $|\omega_j\rangle$ represent single-photon states occupying discrete, well-separated frequency bins. Although some behavior of such a state can be realized in a destructive fashion by using broadband, continuous frequency entanglement and projecting onto separable frequency states during measurement (e.g., as in [21,22]), for most quantum applications it is necessary to use explicitly discrete quantum states that are not components of a broader continuous distribution. There have been some proposals and attempts to create and demonstrate discrete-color entanglement in nonlinear waveguides [24,25] and fiber Sagnac loops [26]. To date, however, no experiment has been able to conclusively show the creation or quantitative characterization of discretely color-entangled photons.

Here we report the first experimental demonstration of genuine discretely color-entangled states, created without any spectrally selective filtering. We used a hybrid quantum gate, a gate that acts simultaneously on different DOFs, that can deterministically transfer polarization onto color entanglement and unambiguously verified and quantified this entanglement using nonclassical interference. We also demonstrated full control over the frequency separation and phase of the created states, while maintaining a high fidelity.

In our experiment (Fig. 1), a tunable source of polarization entanglement based on continuous-wave SPDC [4] generates fiber-coupled photon pairs close to a pure state:

$$|\psi_{\text{in}}\rangle = (\alpha|H\rangle_1|H\rangle_2 + e^{i\phi}\beta|V\rangle_1|V\rangle_2) \otimes |\omega_1\rangle_1|\omega_2\rangle_2, \quad (1)$$

where $\alpha^2 + \beta^2 = 1$, $H$ and $V$ denote vertical and horizontal polarization, and $\omega_j$ is the central frequency of mode $j$. This notation neglects the spectral entanglement within the single-photon bandwidth, which was much less than the photons' frequency separation, $\mu = \omega_1 - \omega_2$. By varying the temperature of the source's nonlinear crystal (periodically poled potassium titanyl phosphate, ppKTP), we continuously tuned the photon frequencies from degeneracy

 

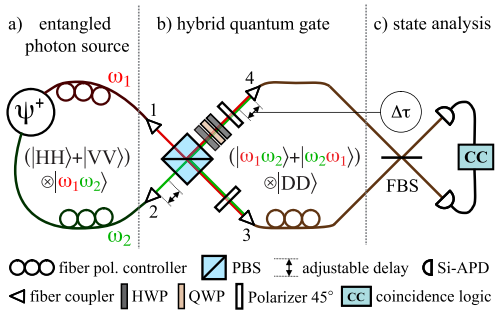


FIG. 1 (color online). Schematic of the experimental setup. (a) Source of polarization-entangled photon pairs with tunable central frequencies. (b) The hybrid quantum gate's polarizing beam splitter (PBS) maps the polarization entanglement onto the color degree of freedom. Subsequently projecting on diagonal (D) polarization with polarizers (POL) generates the discretely color-entangled state. (c) The state is analyzed by two-photon interference at a fiber beam splitter (FBS); Si-APD single-photon detectors and coincidence counting (CC) logic measure the coincidence rate as a function of temporal delay between modes.

(809.6 nm at 25.1 °C) to a maximum separation of 8.4 THz (18.3 nm) at 68.1 °C while maintaining high-quality polarization entanglement [4]. We controlled the polarization state with wave plates.

Single mode fibers connect the source to the inputs of the hybrid gate depicted in Fig. 1(b). The polarizing beam splitter (PBS) maps the state $|\omega_1\rangle_1$, depending on its polarization, to $|\omega_1\rangle_3$ ($H$) or $|\omega_1\rangle_4$ ($V$), and similarly for the state $|\omega_2\rangle_2$. This transfers the existing polarization entanglement onto color with the resulting *hypoentangled* [27,28] multi-DOF state:

$$|\psi_{\text{hypo}}\rangle = \alpha|H\omega_1\rangle_3|H\omega_2\rangle_4 + e^{i\phi}\beta|V\omega_2\rangle_3|V\omega_1\rangle_4. \quad (2)$$

To create the desired state, the frequency entanglement must then be decoupled from the polarization DOF. This can be achieved deterministically by selectively rotating the polarization of one of the two frequencies (e.g., using dual-wavelength wave plates). For simplicity, we instead chose to erase the polarization information probabilistically by projecting both photons onto diagonal polarization using polarizers at 45°. We erased temporal distinguishability between input photons by translating fiber coupler 2 to maximize the nonclassical interference visibility at the PBS for degenerate photons. Finally, we compensated for unwanted birefringent effects of the PBS using wave plates in one arm. The gate output is then:

$$|\psi_{\text{out}}\rangle = \alpha|\omega_1\rangle_3|\omega_2\rangle_4 + e^{i\phi}\beta|\omega_2\rangle_3|\omega_1\rangle_4. \quad (3)$$

The parameters defining this state can be set by preparing an appropriate polarization input state [Eq. (1)].

To explore the performance of the hybrid gate, we first injected photon pairs close to the polarization state $(|H\rangle_1|H\rangle_2 - |V\rangle_1|V\rangle_2)/\sqrt{2}$ with individual wavelengths 811.9 and 807.3 nm. The gate should then ideally produce the discrete, anticorrelated color-entangled state: $|\psi\rangle = (|\omega_1\rangle_3|\omega_2\rangle_4 - |\omega_2\rangle_3|\omega_1\rangle_4)/\sqrt{2}$. Figure 2(a) shows the unfiltered single-photon spectra of the two output modes, illustrating that each photon is measured at either $\omega_1$ or $\omega_2$. This reflects a curious feature of discretely color-entangled states, that individual photons have no well-defined color and no photon is ever observed at the "mean-value" frequency. This is one of the features that clearly distinguishes our experiment from the continuous frequency entanglement studied in Refs. [5,21,22].

Because the detuning, $\mu = 4.6$ nm, is much larger than the FWHM bandwidth of the individual color modes of 0.66 nm (0.30 THz; defined by the 10 mm nonlinear crystal), the two modes are truly orthogonal, making them good logical states for a frequency-bin qubit. This orthogonality also means that color anticorrelations are strictly enforced by energy conservation, because a single down-conversion event cannot produce two photons in the same frequency bin. We confirmed this by directly measuring the gate output in the frequency-bin computational basis (i.e., with coarse-scale 2 nm-wide filtering in each arm at either $\omega_1$ or $\omega_2$). We observed strong, comparable coincidence rates for the two "anticorrelated" basis states (10 882 ± 104 and 9068 ± 95 in 30 s for $|\omega_1\rangle_3|\omega_2\rangle_4$ and $|\omega_2\rangle_3|\omega_1\rangle_4$, respectively), and no coincidences for the same-frequency states ($|\omega_1\rangle_3|\omega_1\rangle_4$ and $|\omega_2\rangle_3|\omega_2\rangle_4$) to within error bars determined by the filters' finite extinction ratios.

To demonstrate that the color state was not only anticorrelated but genuinely entangled, we used nonclassical two-photon interference [29], overlapping the photons at a 50:50 fiber beam splitter (FBS) [Fig. 1(c)] and varying their relative arrival time by translating fiber coupler 4 while observing the output coincidences. The results in

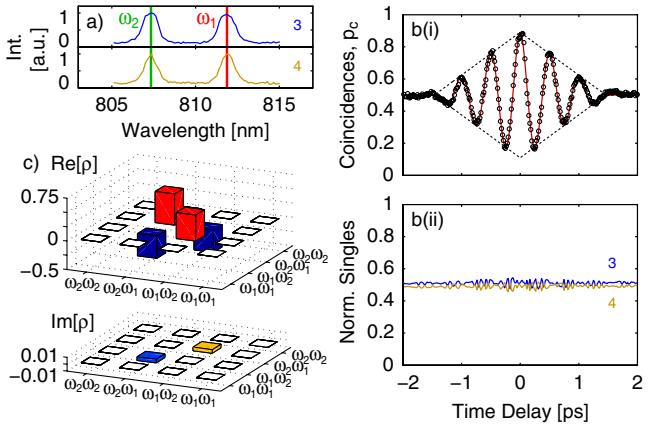


FIG. 2 (color online). Analysis of the discretely color-entangled state. (a) Single-photon spectra for modes 3 and 4; frequency separation is 2.1 THz (4.6 nm). The observed width of each bin is limited by the single-photon spectrometer. (b) Normalized (i) coincidence and (ii) singles count rates as a function of delay in mode 4. The solid line in (i) is a fit of Eq. (5) to determine $V$ and the phase $\phi$. (c) The estimated restricted density matrix: target-state fidelity, 0.891 ± 0.003; tangle, 0.611 ± 0.009; and purity, 0.801 ± 0.004.

Fig. 2(b) show high-visibility sinusoidal oscillations (frequency $\mu$) within a triangular envelope caused by the *unfiltered* "sinc-squared" spectral distribution of the source [4], whereas the single-photon detection rates exhibit negligible interference effects. At the central delay, the normalised coincidence probability reaches up to $0.881 \pm 0.007$, far above ($>50\sigma$) the baseline level of 0.5. This two-photon antibunching is an unambiguous signature of antisymmetric entanglement [23,30,31] and, in conjunction with the measured single-photon spectra, conclusively demonstrates that we have created a truly discrete-color state that is strongly entangled. We emphasize again that our measurements do not rely on any spectrally selective filtering, but result from directly generated discrete color entanglement.

On its own, our measured nonclassical fringes are similar to those observed in previous work on frequency entanglement. However, as demonstrated by Kaltenbaek *et al.* [32], observing such a signal in different contexts cannot always lead to the same conclusions. In earlier experiments [21,22], the observed signal resulted from broadband, continuous frequency entanglement which was projected onto separable frequency states during measurement. At no point could the quantum state of the photons be described as both a discrete-color and a color-entangled state, as well as being uncoupled from other DOFs. In more recent work [26], Li and co-workers produced and verified high-quality continuous color entanglement using a Sagnac-based source. In principle, such a configuration might also produce discrete color entanglement, but their filter-based measurements alone would not be able to discriminate this from the continuous case.

We now show how we can combine the above measurements to estimate a restricted density matrix in color space. We first recall that energy conservation in the SPDC pair source and during photon propagation constrains the state to the two-dimensional anticorrelated subspace of the two-qubit color space (before and after the gate). This is a physical constraint, validated by the measurements in the computational basis. The complete density matrix within this subspace can be written (in the computational basis, $\{|\omega_1\rangle_3|\omega_1\rangle_4, |\omega_1\rangle_3|\omega_2\rangle_4, |\omega_2\rangle_3|\omega_1\rangle_4, |\omega_2\rangle_3|\omega_2\rangle_4\}$):

$$\rho = \begin{pmatrix} 0 & 0 & 0 & 0 \\ 0 & p & \frac{V}{2}e^{-i\phi} & 0 \\ 0 & \frac{V}{2}e^{i\phi} & 1-p & 0 \\ 0 & 0 & 0 & 0 \end{pmatrix} \tag{4}$$

with real parameters that obey the physicality constraints: $0 \le p \le 1$ and $0 \le \frac{V}{2} \le \sqrt{p(1-p)}$. Any detection events outside this subspace arise from higher-order emissions and accidental coincidences, and also lie outside the full two-qubit space. Our computational basis measurements showed that these vanished to within error bars, and we directly calculated the balance parameter, $p = 0.546 \pm 0.004$ (using Poissonian errors). We estimated the remaining parameters by fitting them to the nonclassical interference signal. For the above density matrix, given the source's spectral properties, we analytically calculated the expected interference probability, $p_c$, to be (following [23])

$$p_c(\tau) = \tfrac{1}{2} - \tfrac{V}{2}\cos(\mu\tau + \phi)(1 - |\tfrac{2\tau}{\tau_c}|) \quad \text{for } |\tau| < \tfrac{\tau_c}{2}, \tag{5}$$

where the coherence time $\tau_c$ is the base-to-base envelope width, related to the single-photon frequency bandwidth via $\Delta f_{\mathrm{FWHM}} = 0.885/\tau_c \sim 0.3$ THz. The missing elements $V$ and $\phi$ can be identified as the visibility and phase of the oscillating signal and can therefore be estimated using curve fitting (for this state, $V = 0.782 \pm 0.006$ and $\phi = 179.2 \pm 0.4°$). The resulting density matrix [Fig. 2(c)] is strongly entangled, with a target-state fidelity of $0.891 \pm 0.003$, tangle [33] of $0.611 \pm 0.009$, and purity of $0.801 \pm 0.004$ (error bars include Poissonian and fitting errors). This is the first quantitative measurement of the entanglement of any color-entangled state.

Several error sources in our experiment contributed cumulatively to unwanted photon distinguishability in the final color state and reduced the measured entanglement, including imperfect input polarization states, imperfect mode matching and residual polarization misalignment at the PBS, the finite PBS extinction ratio, and a slightly asymmetric FBS splitting. Accidental coincidence counts caused by detector dark counts and higher-order SPDC contributions were negligible.

To illustrate the flexibility of the hybrid gate, we analyzed a series of output states for different frequency detunings $\mu$ and phases $\phi$. We first tuned $\mu$ by varying the crystal temperature in the source, and the results (Fig. 3) agree well with Eq. (5). The source enabled us to reach a detuning of 18.3 nm (8.4 THz), about 30 times the individual color-bin bandwidths. The detunings estimated from curve fitting matched the single-photon spectra.

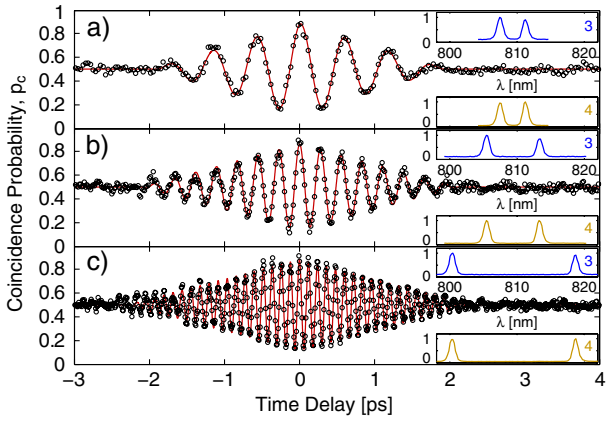


FIG. 3 (color online). Two-photon interference for color-entangled states with three different frequency separations (and corresponding crystal temperatures): (a) 1.7 THz (3.8 nm), 33.7 °C; (b) 3.6 THz (7.9 nm), 43.7 °C; and (c) 8.4 THz (18.3 nm), 68.1 °C. Solid lines are fits to Eq. (5) with $V$, $\mu$, and $\phi$ as fitting parameters. The insets show the measured single-photon spectra for both modes of each state.

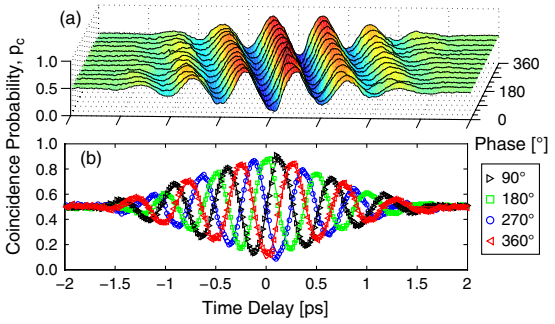


FIG. 4 (color online). (a) Coincidence probabilities after the FBS as a function of the delay for 13 close-to-maximally entangled discrete color states. The phase of the oscillation pattern is proportional to the phase of the original polarization-entangled state. (b) Four close-to-maximally entangled discrete-color states that represent two unbiased bases.

We next prepared discrete-color states of the form $(|\omega_1\rangle_3|\omega_2\rangle_4 + e^{i\phi}|\omega_2\rangle_3|\omega_1\rangle_4)/\sqrt{2}$ with varying phase ($\phi = 0°, 30°, \ldots, 360°$) (Fig. 4). The measured states display an average target-state fidelity of $0.90 \pm 0.01$, a tangle of $0.63 \pm 0.03$, and a purity of $0.82 \pm 0.02$, demonstrating that the hybrid gate accurately preserves quantum information stored in the original polarization state. Note that, together with the product states $|\omega_1\rangle_3|\omega_2\rangle_4$ and $|\omega_2\rangle_3|\omega_1\rangle_4$, the entangled states with phase 0°, 90°, 180°, and 270° constitute a full set of qubit mutually unbiased bases. This illustrates the states' potential usefulness for quantum protocols such as quantum cryptography.

In this Letter, we have for the first time conclusively demonstrated the creation, control, and characterization of high-quality, discretely color-entangled states, prepared without any spectrally selective filtering using a hybrid quantum gate. We performed the first quantitative measurement of color entanglement using a novel technique for characterizing the two-qubit color state within a restricted, antisymmetric subspace defined by energy conservation. Our hybrid gate can in fact be used to transfer polarization entanglement onto any desired photonic DOF ($\xi$), by preparing the input $|\psi\rangle_{\mathrm{pol}} \otimes |\xi_1, \xi_2\rangle$ and by appropriately erasing the polarization information after the PBS. Because the preparation of high-quality polarization states can be much easier than in other photonic DOFs, this gate represents a valuable tool for quantum information processing tasks in those DOFs. Our work also has important implications for the development of quantum memories and repeaters, because color-encoded information could provide a natural interface between flying and stationary qubits (such as single ions, atoms, or atom ensembles) where information is encoded in different energy levels. Indeed, by inverting the procedure from [14], one could potentially entangle distant ions directly by letting them absorb a photon pair with the appropriate discrete-color entanglement. Finally, we point out that genuine, discretely color-entangled states could also be extracted nondeterministically from broadband sources of continuous spectral entanglement (such as traditional SPDC) using custom-designed multiband bandpass filters. This is a fundamentally different approach from previous experiments, where some signatures of discrete-color entanglement were reproduced by projecting onto discrete, separable states during measurement using single-band bandpass filters. Although this novel alternative would not be easily tunable and efficient, as ours is, it would allow access to higher-dimensional entangled states in the color DOF.

We would like to thank T. Jennewein and B. Blausteiner and acknowledge support from the FWF (SFB 015 and CoQuS), the E.C. Project QAP, and the DTO-funded U.S. Army Research Office QCCM program.

[1] P. G. Kwiat *et al.*, Phys. Rev. Lett. **75**, 4337 (1995).
[2] P. G. Kwiat *et al.*, Phys. Rev. A **60**, R773 (1999).
[3] T. Kim, M. Fiorentino, and F. N. C. Wong, Phys. Rev. A **73**, 012316 (2006).
[4] A. Fedrizzi *et al.*, Opt. Express **15**, 15 377 (2007).
[5] P. G. Kwiat, A. M. Steinberg, and R. Y. Chiao, Phys. Rev. A **47**, R2472 (1993).
[6] J. Brendel *et al.*, Phys. Rev. Lett. **82**, 2594 (1999).
[7] J. G. Rarity and P. R. Tapster, Phys. Rev. Lett. **64**, 2495 (1990).
[8] A. Mair *et al.*, Nature (London) **412**, 313 (2001).
[9] N. K. Langford *et al.*, Phys. Rev. Lett. **93**, 053601 (2004).
[10] M. de Burgh and S. D. Bartlett, Phys. Rev. A **72**, 042301 (2005).
[11] V. Giovannetti, S. Lloyd, and L. Maccone, Nature (London) **412**, 417 (2001).
[12] L. Xiao *et al.*, Phys. Rev. A **77**, 042315 (2008).
[13] O. Minaeva *et al.*, Phys. Rev. Lett. **102**, 100504 (2009).
[14] S. Olmschenk *et al.*, Science **323**, 486 (2009).
[15] M. Fujiwara *et al.*, Phys. Rev. Lett. **90**, 167906 (2003).
[16] C. Wang *et al.*, Phys. Rev. A **71**, 044305 (2005).
[17] D. Bruss and C. Macchiavello, Phys. Rev. Lett. **88**, 127901 (2002).
[18] N. J. Cerf *et al.*, Phys. Rev. Lett. **88**, 127902 (2002).
[19] R. W. Spekkens and T. Rudolph, Phys. Rev. A **65**, 012310 (2001).
[20] S. Kochen and E. P. Specker, J. Math. Mech. **17**, 59 (1967).
[21] J. G. Rarity and P. R. Tapster, Phys. Rev. A **41**, 5139 (1990).
[22] Z. Y. Ou and L. Mandel, Phys. Rev. Lett. **61**, 54 (1988).
[23] A. Fedrizzi *et al.*, New J. Phys. **11**, 103052 (2009).
[24] M. C. Booth *et al.*, Phys. Rev. A **66**, 023815 (2002).
[25] M. Ravaro *et al.*, J. Appl. Phys. **98**, 063103 (2005).
[26] X. Li *et al.*, Phys. Rev. A **79**, 033817 (2009).
[27] N. K. Langford, Ph.D. thesis, Univ. of Queensland, 2007.
[28] X.-F. Ren *et al.*, Chin. Phys. Lett. **23**, 552 (2006).
[29] C. K. Hong, Z. Y. Ou, and L. Mandel, Phys. Rev. Lett. **59**, 2044 (1987).
[30] K. Mattle *et al.*, Phys. Rev. Lett. **76**, 4656 (1996).
[31] K. Wang, J. Phys. B **39**, R293 (2006).
[32] R. Kaltenbaek, J. Lavoie, and K. J. Resch, Phys. Rev. Lett. **102**, 243601 (2009).
[33] V. Coffman, J. Kundu, and W. K. Wootters, Phys. Rev. A **61**, 052306 (2000).